PHILOSOPHICAL TRANSACTIONS OF THE ROYAL SOCIETY A MATHEMATICAL, PHYSICAL & ENGINEERING SCIENCES

Dimensional Changes in Pyrolytic Graphite under Fast-Neutron Irradiation

B. T. Kelly, W. H. Martin and P. T. Nettley

Phil. Trans. R. Soc. Lond. A 1966 **260**, 37-49
doi: 10.1098/rsta.1966.0028

DIMENSIONAL CHANGES IN PYROLYTIC GRAPHITE UNDER FAST-NEUTRON IRRADIATION

By B. T. KELLY, W. H. MARTIN and P. T. NETTLEY
United Kingdom Atomic Energy Authority, Reactor Materials Laboratory, Culcheth, Warrington, Lancs.

(*Communicated by H. Kronberger, F.R.S.—Received 4 October 1965—Read 3 March 1966*)

[Plate 1]

CONTENTS

Measurements are reported of the principal strains and changes in principal thermal expansion coefficients of various grades of pyrolytic graphite after fast-neutron bombardment at constant temperatures in the range 150 to 650 °C. The pyrolytic graphites used in these studies possess properties approaching those of a monocrystal and the irradiation effects observed thus closely represent those expected in a crystal.

The observations are compared with previous inferences of the behaviour of crystals in less well oriented polycrystalline materials under the same irradiation conditions and are discussed in terms of recent theories of the accumulation of irradiation damage in fast-neutron irradiated graphite. The existence of a new type of vacancy configuration is postulated to explain the crystal dimensional changes at high doses and high temperatures. A qualitative explanation of the changes in crystal thermal expansion coefficients is proposed.

1. Introduction

The understanding of the dimensional changes produced in nuclear polycrystalline graphites by fast-neutron irradiation must be preceded by knowledge of the behaviour of graphite monocrystals under the same irradiation conditions. Previous work by the United Kingdom Atomic Energy Authority has concentrated upon the deduction of the behaviour of monocrystals from results obtained on polycrystalline graphites together with some measurements of dimensional changes on small natural graphite crystals after irradiation at 200 °C (Simmons 1957; Simmons & Reynolds 1962; Goggin, Henson, Perks & Reynolds 1964; Bridge, Kelly & Nettley 1964).

The production of highly oriented pyrolytic graphite (cf. Brown, Watt, Powell & Tye 1956; Blackman, Saunders & Ubbelohde 1961; Diefendorf 1960) with properties very close to those of monocrystals allows the direct measurement of the effects of fast-neutron irradiation on the dimensions and principal thermal expansion coefficients of essentially single crystals.

Vol. 260. A. 1109. (Price 15s.; U.S. $2.25) 5 [Published 16 June 1966

This paper reports the results of such a study in the range of irradiation temperatures 150 to 650 °C. The application of these results to the interpretation of dimensional changes in a polycrystalline aggregate is discussed in the succeeding paper.

2. Experimental

Materials

The studies described in this paper employed three distinct types of pyrolytic graphite.

The first type, designated α, was obtained from High Temperature Materials Inc. U.S.A., in the as-deposited condition. The deposition was performed from the gas phase onto a graphite substrate at a temperature of 2100 to 2200 °C. The material was received in the form of plates approximately 4 in. square and $\frac{1}{4}$ in. thick possessing a bulk density of 2·2 g/cm^3.

The second type of material, denoted by β, was prepared from the α type by heat treatment at 2900 °C for 1 h in an inert gas atmosphere. This treatment improved the crystal perfection and orientation of the material.

The third material, denoted by γ, was obtained through the courtesy of Dr R. Diefendorf of the General Electric Company of the U.S.A. This sample was prepared by annealing at 3300 to 3600 °C and its appearance corresponded closely to that of natural single crystals except that it was much larger, in the form of a plate approximately 1 in. square and $\frac{1}{8}$ in. thick.

The available physical properties and X-ray parameters of these materials are collected in table 1, and compared with the best available properties of monocrystals. The chemical purity of each of these materials has been checked by the Chemical Services Department of the Capenhurst Works, U.K.A.E.A. Production Group; the only significant impurities are a few parts per million of iron, silicon and boron. The levels are well below those expected to cause the nucleation of irradiation defects which has been observed by Thrower (1964).

The X-ray parameters entered in table 1 are:

L_a the average diameter of a layer network over which there is considerable perfection;
L_c the total height irrespective of turbo-stratic stacking of a parallel layer group;
d_{002} the interlayer spacing;
P the probability of finding adjacent layers incorrectly stacked; and
ϕ the semi-vertical angle of the cone with axis normal to the deposition plane which will contain at least 95 % of the c axes of the constitutent crystallites.

The structure of such materials at a coarser level is described by Tarpinian (1962) and Bragg, Crooks, Fenn & Hammond (1964).

Transmission electron micrographs were obtained from the β and γ materials and a single crystal obtained from the Ticonderoga source (Freise & Kelly 1961), the electron beam in each case passing along the normal to the basal planes, with the observations being made in bright field. These micrographs are shown in figure 1, plate 1. No transmission could be obtained in the α material.

Table 1 illustrates two important conclusions; first that in order of increasing perfection:

α material corresponds to the perfection of a poorly graphitized soft carbon;
β material corresponds to the perfection of a well crystallized reactor graphite;
γ material corresponds to the perfection of the best monocrystals available;

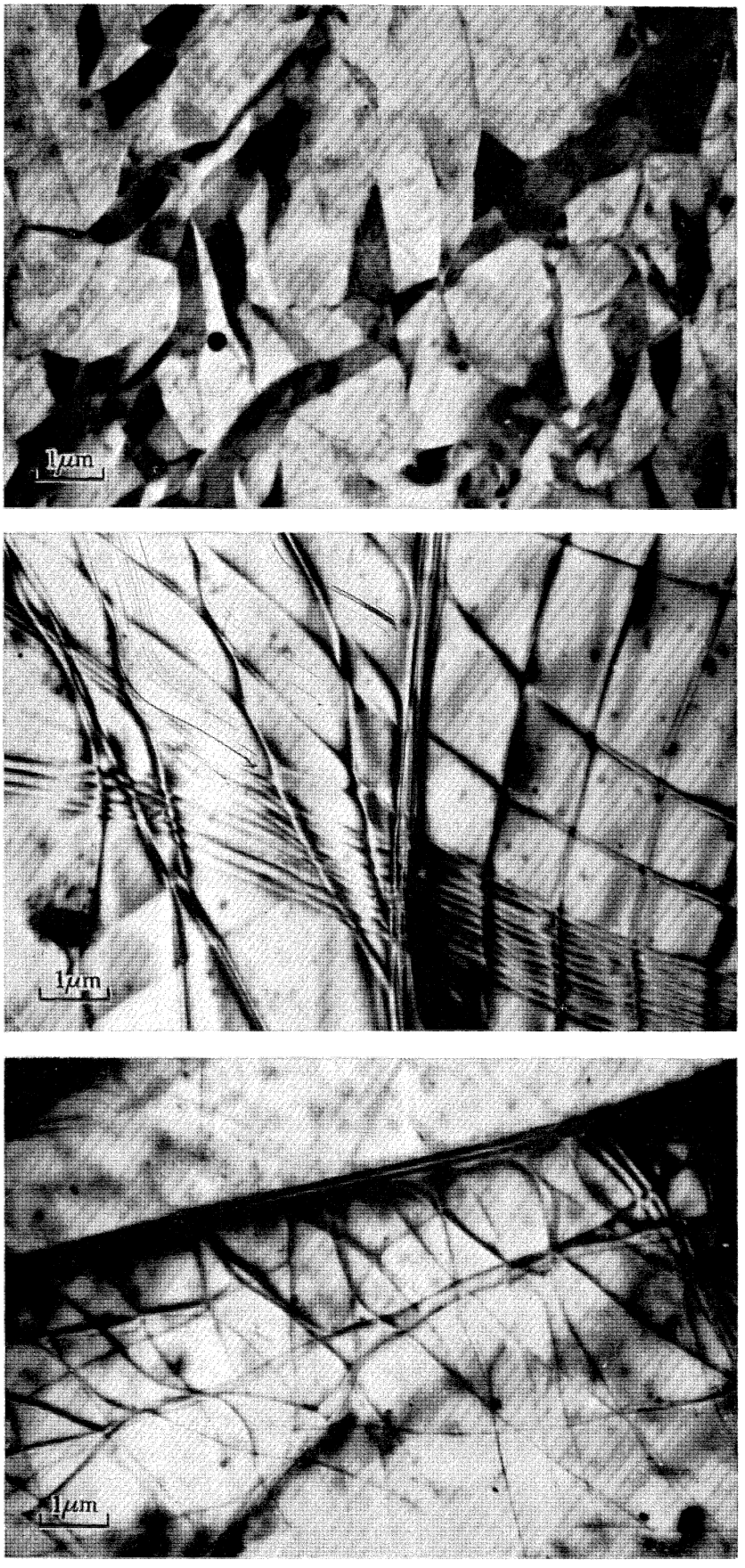

(A) β type material

(B) γ type material

(C) Ticonderoga flake graphite

FIGURE 1. Transmission electron micrographs of pyrolytic and monocrystalline graphite. (Magn. $\times 8700$). Micrographs (B) and (C) show dislocation networks lying in the basal planes.

(*Facing p.* 38)

PHILOSOPHICAL TRANSACTIONS OF THE ROYAL SOCIETY A MATHEMATICAL, PHYSICAL & ENGINEERING SCIENCES

PHILOSOPHICAL TRANSACTIONS OF THE ROYAL SOCIETY A MATHEMATICAL, PHYSICAL & ENGINEERING SCIENCES

Table 1. Properties of the materials investigated

source	designation	X-ray parameters L_c (Å)	L_a (Å)	d_{002} (Å)	ϕ (deg)	P	physical properties: electrical resistivity (20 °C) (Ω cm) 'a'	'c'	thermal expansion (20 to 120 °C) (degC^{-1}) 'a'	'c'	thermal conductivity (20°C) (cal cm^{-1} s^{-1} degC^{-1}) 'a'	'c'	comments
high temperature materials	α	< 200*	< 100*	3·425* 3·421*	40 ± 5*	0·95*	$20{\cdot}0\times10^{-5}$†	—	$+0{\cdot}5\times10^{-6}$†	20×10^{-6}†	0·68†	0·0047†	as deposited at 2150 °C
high temperature materials	β	~1000*	~1000*	3·356* 3·361†	~ 7	~ 0·1*	$5{\cdot}3\times10^{-5}$†	1·05†	$-0{\cdot}9\times10^{-6}$†	$24{\cdot}6\times10^{-6}$†	2·69†	0·014†	α material heat treated to 2900 °C
General Electric Co.	γ	∞	∞	3·354†	~ 0*†	0†	—	—	—	$25{\cdot}0\times10^{-6}$†	3·6†	0·017†	strain annealed 3300 to 3600 °C
natural crystals	—	∞	∞	3·354§	—	0§	$3{\cdot}8\times10^{-5}$‖	0·5–1·0¶	$-1{\cdot}5\times10^{-6}$**	$27{\cdot}0\times10^{-6}$**	~ 2††	—	from Ticonderoga source

In columns 8 to 14 'a' refers to measurements along, and 'c' normal to, the basal planes of the crystals in the sample.

* Measurements made by Kellett, Wallace & Richards (1962–64).
† Measurements made at Reactor Materials Laboratory, Culcheth.
§ Freise & Kelly (1961).
‖ Primak & Fuchs (1954).
¶ Taken from Ubbelohde & Lewis (1960).
** Nelson & Riley (1945).
†† Smith (1956).

secondly, that the principal strains (normal and parallel to the deposition plane) closely represent in each material the strains of a monocrystal in the *c* axis and *a* axis directions. This is clear from a comparison of the principal thermal expansion coefficients of each grade with those of the monocrystal.

Samples were cut from each material in the form of cylinders 0·2 in. in diameter with axes parallel or perpendicular to the plane of the plates. The γ material samples cut parallel to the plane of the plate could not usually be used for measurements of any kind due to the easy cleavage along the basal planes. The susceptibility of this material to damage necessitated the use of an Airbrasive cutting tool which uses a jet of abrasive particles to erode unwanted material; the specimen shaping was achieved by means of stainless steel templates of the required shape.

The end faces of the α and β material cylinders were polished to a flatness of $\pm 5\,\mu$in.; this treatment was not possible for the γ material owing to its fragility; however, its surfaces were adequate for measurements normal to the plane of the plate.

Irradiation techniques

Irradiation was performed in specially designed temperature controlled furnaces located in the cores of the heavy water moderated Materials Testing Reactors DIDO and PLUTO at the Atomic Energy Research Establishment, Harwell.

The irradiation equipment and the furnace design used for these studies have been described by Bell, Bridge, Cottrell, Greenough, Reynolds & Simmons (1962) in a previous communication, and are not further described here. The essential features of the irradiation facility are the provision of identical neutron spectra for each irradiation and the maintenance of close control of sample temperatures.

The fast-neutron dose is expressed in terms of the reaction $^{58}\mathrm{Ni}(n,p)^{58}\mathrm{Co}$ for a cross-section of 107 mb (cf. Martin & Clare 1964). The instantaneous fast-neutron flux in these irradiations varied from 3×10^{13} to 7×10^{13} n cm^{-2} s^{-1}.

The irradiation temperatures were controlled automatically to ± 2 degC for the irradiations conducted below 300 °C and to ± 10 degC above this temperature. The small samples were contained in thin walled aluminium or stainless steel capsules to ensure their safety in remote handling during unloading of the furnace. The actual sample temperatures are somewhat higher than the nominal temperature, due to the nuclear heating in graphite in these facilities. Calculations for the solid graphite samples used by Bell *et al.* showed that the correction lay in the range 0 to $+10$ degC of the nominal temperature. This range is expected to be 0 to $+15$ °C for the present samples because of the presence of the surrounding canning material.

Measurement techniques

The dimensional changes were measured with a Sigma comparator to determine the differences in lengths between a standard steel slip gauge and the sample before and after irradiation. To prevent mechanical deformation of the samples due to the load of the comparator probe, an optically flat quartz block, on one face of which were etched parallel line contacts, was interposed between the comparator probe and sample and the sample and comparator baseplate. The same quartz blocks were used during the standard length

measurements and their thicknesses were thus eliminated in difference measurements. The length measurements are accurate to ± 50 parts in a million at all doses.

The thermal expansion coefficients were measured over the range 20 to 120 °C with either a Fizeau interferometer (McFarlane 1965) or a silica tube dilatometer. The measurements normal to the deposition plane are accurate to $\pm 1 \times 10^{-6}\,\mathrm{degC}^{-1}$ and those parallel to the deposition plane to $\pm 0{\cdot}2 \times 10^{-6}\,\mathrm{degC}^{-1}$.

3. Results

The dimensional changes observed perpendicular to the plate (c axis direction) and parallel to the plate (a axis direction) in β type material are presented in figure 2 for irradiations at 150, 170, 200 and 250 °C, while figure 3 presents dimensional changes in the same material for irradiations at 300, 350, 450 and 650 °C nominal furnace temperatures.

The effect of irradiation on the principal thermal expansion coefficients, α_c and α_a, of the β material is presented in figures 4 and 5, while figures 6 and 7 compare the dimensional change and thermal expansion behaviour of the α, β and γ materials at a temperature of 170 °C. The fragility of the γ material precluded dimensional change or thermal expansion measurements along the plane of the plate.

It should be noted that a distinction is made in the β material between samples prepared from two separate plates of α material, known as 1 and 4. The thermal expansion data (figures 6 and 7) show that plate 4 is slightly less well oriented and more variable than plate 1; this does not affect the significance of these results and is not referred to again in this paper.

4. Discussion

The close correspondence of the principal thermal expansion coefficients of the pyrolytic graphite to the c axis thermal expansion coefficient α_c and the a axis thermal expansion coefficient α_a of a perfect graphite crystal show that we may consider, in agreement with the conclusions of Entwisle (1962), that any strain measured normal to and parallel to the deposition plane approximates very closely to the strains in the c axis and a axis directions respectively of a crystallite of the material.

The results at each irradiation temperature may be compared with the crystal dimensional changes and changes in crystal thermal expansion coefficients deduced from results on less well oriented polycrystalline graphites by Goggin *et al.* (1964) and Brocklehurst & Weeks (1963). The results at 200 °C confirm the increase in the rates of change of crystal dimensions with dose reported by these authors at *ca.* $4 \times 10^{20}\,\mathrm{n/cm^2}$ in samples irradiated under the same conditions as the present experiment. The irradiation induced changes in thermal expansion coefficients deduced by these authors at the same temperature differ in detail from the present observations, but they must be regarded as less definitive since they were indirect deductions from less well oriented polycrystalline graphite behaviour. At irradiation temperatures in excess of 300 °C no change in thermal expansion coefficients is observed in the dose range investigated, again in agreement with the less well oriented polycrystalline graphite data (Simmons, Kelly, Nettley & Reynolds 1964). A particularly important point of agreement is illustrated in figures 2 and 3 where lattice parameter measurements on less well oriented polycrystalline samples given by Goggin *et al.* and Kelly, Jones & James (1962) at 200, 450 and 650 °C are shown to be much smaller than the directly

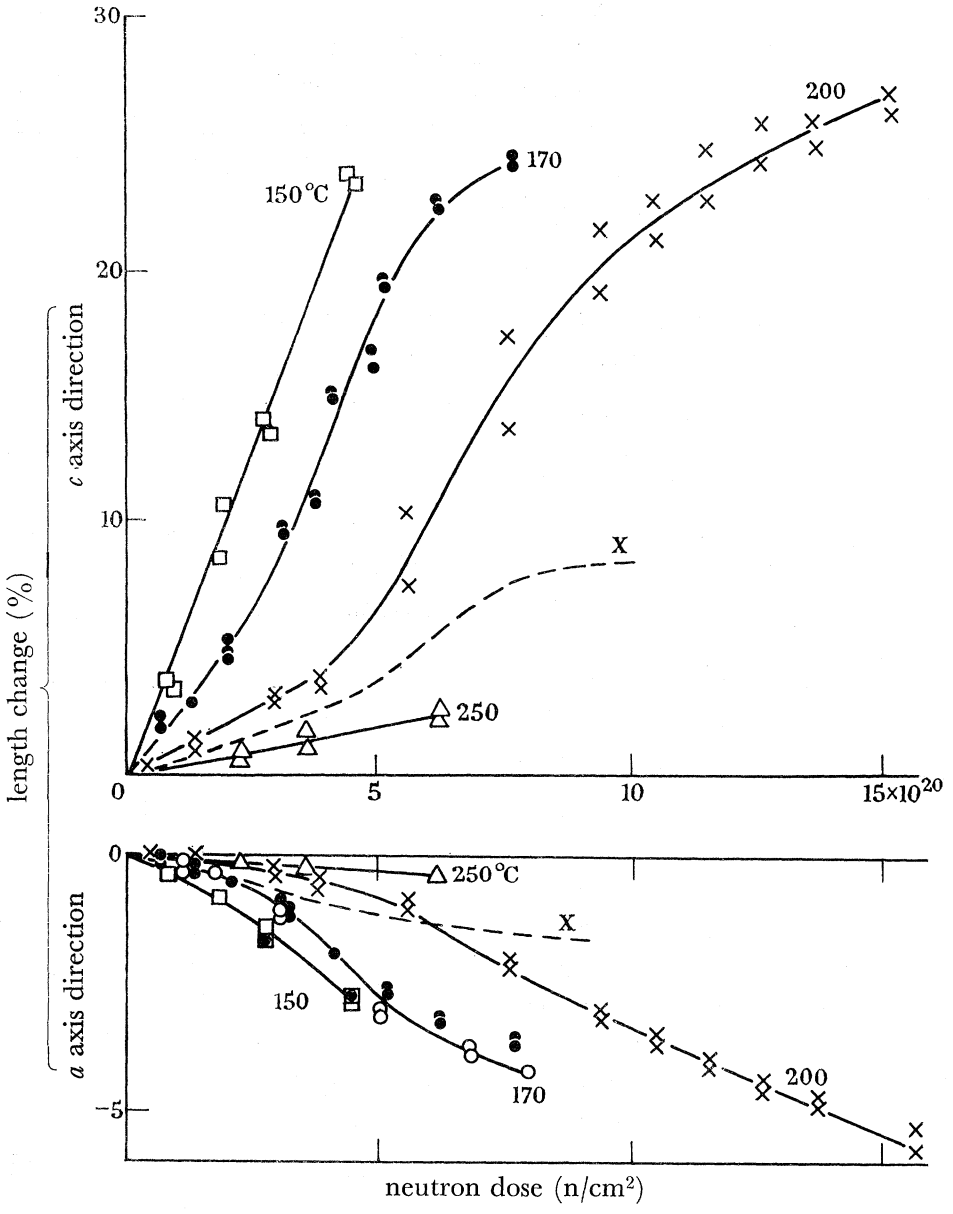

FIGURE 2. Dimensional changes of β type pyrolytic graphite irradiated at 150, 170, 200 and 250 °C perpendicular (c axis direction) and parallel (a axis direction) to the deposition plane.

150 °C	170 °C	200 °C	250 °C
□ plate 1	○ plate 1	× plate 1	△ plate 1
■ plate 4	● plate 4		

X, X-ray results, 200 °C (Goggin *et al.* 1964).

measured crystal strains at the higher doses. It is of interest to note that figure 6 shows that at 170 °C the perfection of the pyrolytic material does not affect the crystal dimensional changes or thermal expansion changes for a given dose significantly, thus indicating the form of the damage to be independent of the crystallite perfection over a considerable range of crystallite size at this temperature. The effect of crystallite size is evidently a complex phenomenon since it has been shown (Kelly, Gray, Martin, Howard, Jenkins & Sørenson 1965) that perfection is important in less well oriented polycrystalline materials which

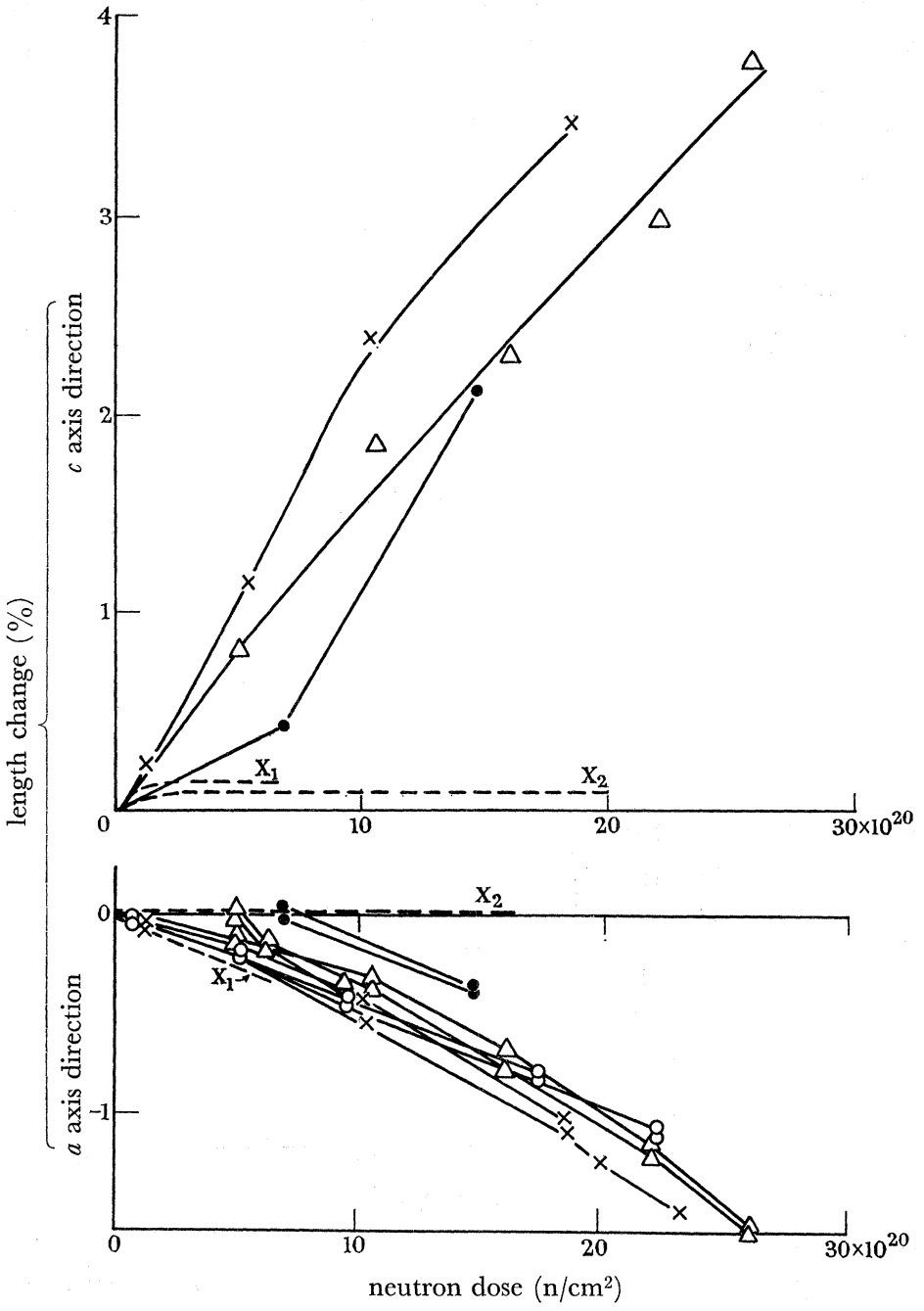

FIGURE 3. Dimensional changes of β type pyrolytic graphite irradiated at 300, 350, 450 and 650 °C perpendicular (c axis direction) and parallel (a axis direction) to the deposition plane. ○, 300 °C; ×, 350 °C; △, 450 °C; ●, 650 °C. X_1, X-ray results, 450 °C (Kelly *et al.* 1962); X_2, X-ray results, 650 °C (Goggin *et al.* 1964).

have very small crystallite size. The observed lack of dependence on crystallite size in pyrolytic material at 170 °C probably arises from the fact that the crystallite size, even in the α material, is large enough for homogeneous nucleation of interstitial defects to occur (Reynolds & Thrower 1963).

The dimensional changes of the graphite crystals are to be attributed to the displaced atoms and vacancies produced by energetic knock-on carbon atoms following the fast-

neutron collisions with carbon nuclei. Each primary knock-on displaces *ca.* 100 atoms, and Simmons (1965) has estimated that in a fast-neutron flux of 4×10^{13} n cm^{-2} s^{-1} (measured by the reaction ^{58}Ni$(n,p)^{58}$Co) the atomic displacement rate is about 10^{-7} atom atom^{-1} s^{-1}. The open crystal structure and low atomic number of carbon lead to the conclusion that

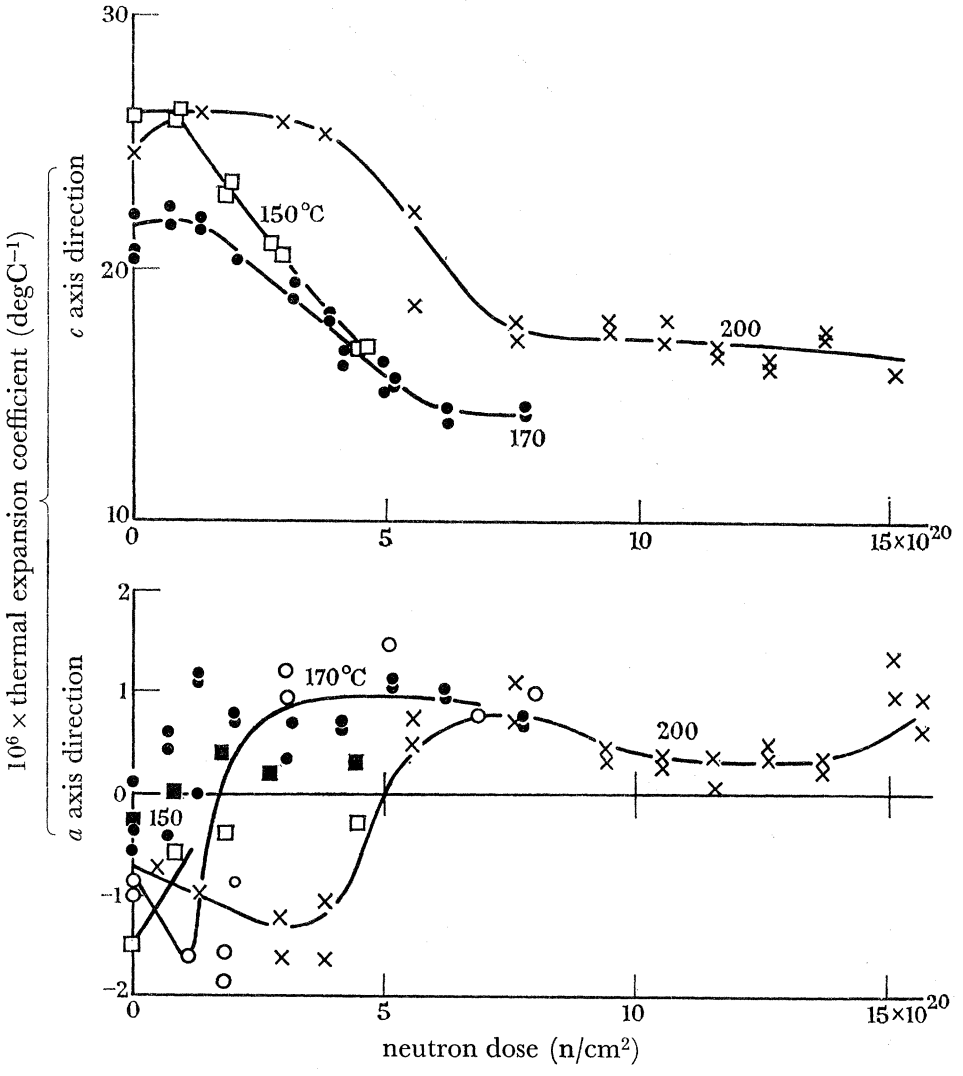

FIGURE 4. Thermal expansion coefficients of β type pyrolytic graphite irradiated at 150, 170 and 200 °C perpendicular (*c* axis direction) and parallel (*a* axis direction) to the deposition plane. The final levels of the *c* axis direction thermal expansion coefficients at the two temperatures coincide well if the plate 4 material is normalized to the more perfect plate 1 initial value.

150 °C	170 °C	200 °C
□ plate 1	○ plate 1	× plate 1
■ plate 4	● plate 4	

these displacements may be considered as randomly generated. The displaced atoms diffuse readily between the layer planes at these temperatures but the vacancies are either immobile or only slightly mobile. The majority of the displaced atoms recombine with vacancies, but the remaining interstitials and vacancies are responsible for the dimensional changes of the graphite crystal and the accompanying physical property changes.

The configuration of the remaining displaced atoms at these temperatures has been described by Reynolds & Thrower (1963) and Simmons *et al.* (1964). Interstitial atoms are believed to be present in two types of configuration: small clusters, each containing about 10 atoms, which do not grow by capturing diffusing interstitial atoms and larger clusters, visible in the electron microscope, which grow continuously by capturing diffusing interstitial atoms. The reason why the small clusters do not grow is not understood but their presence has to be invoked to explain the stored energy release and other physical

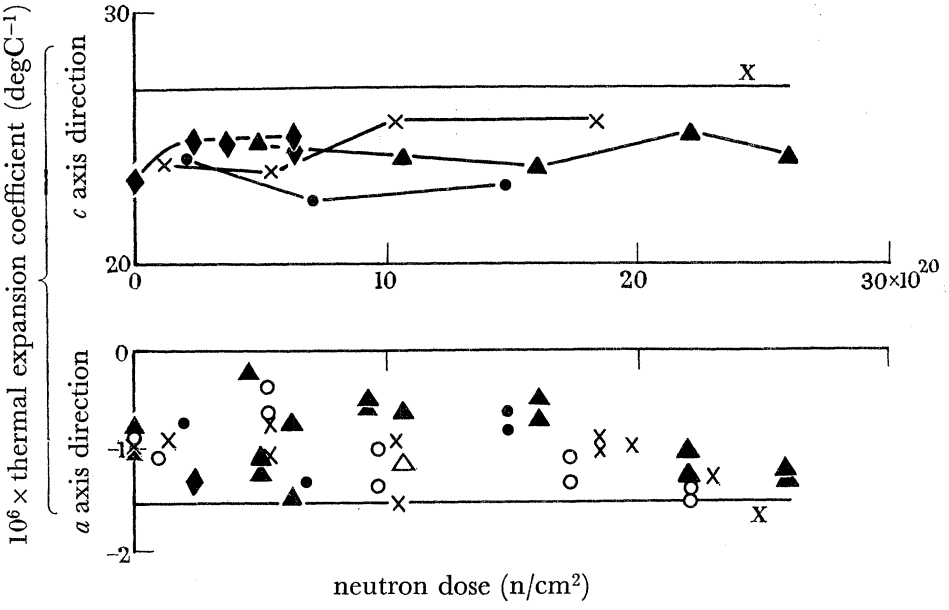

FIGURE 5. Thermal expansion coefficients of β type pyrolytic graphite irradiated at 250, 300, 350, 450 and 650 °C perpendicular (*c* axis direction) and parallel (*a* axis direction) to the deposition plane. ◆, 250 °C; ○, 300 °C; ×, 350 °C; ▲, 450 °C; ●, 650 °C (all plate 1). *X*, Single crystal values (Nelson & Riley 1945).

property changes (Simmons *et al.* 1964). The formation of the larger clusters has been treated in terms of a homogeneous nucleation model (Reynolds & Thrower 1963). The large clusters are essentially small new layer planes, and may be seen to contribute a greater crystal growth in the *c* axis direction than the contribution to *c* axis lattice parameter change (Simmons & Reynolds 1962). The small clusters will make approximately the same contribution to *c* axis growth as to lattice parameter change. The large clusters thus account for the discrepancy between lattice parameter and crystal growth. Comparison of the lattice parameter changes $\Delta c/c$ with the crystal growths shows that at high doses at 200 °C, and for almost all of the dose range at 450 and 650 °C, crystal growth is due to the growth of large interstitial clusters. If we denote the crystal strain in the *c* direction by ϵ_c, then we may write

$$\epsilon_c = \sum_j K_j C_{dj}, \tag{1}$$

where the C_{dj} is the concentration of displaced atoms in the *j*th type of cluster and K_j is an 'importance factor'. The value of K_j is unity for a large interplanar cluster and ~ 5 for a single interstitial atom (Agranovich & Semenov 1964; Kelly 1965). The value of K_j for the small clusters is probably *ca.* 2. These considerations lead to the conclusion that there are 10 to 20 % interstitial atoms at the highest dose in the 200 °C sample.

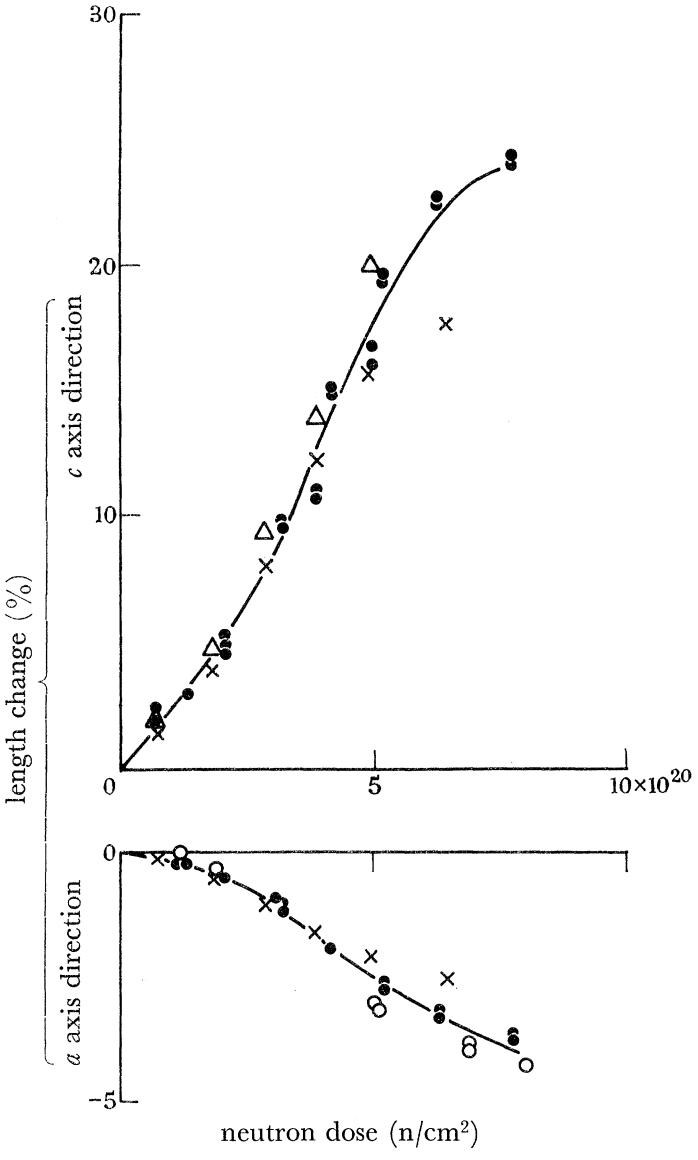

FIGURE 6. Comparison of dimensional changes in α, β and γ pyrolytic graphites irradiated at 170 °C. ×, α material; ○ (plate 1), ● (plate 4), β material; △, γ material.

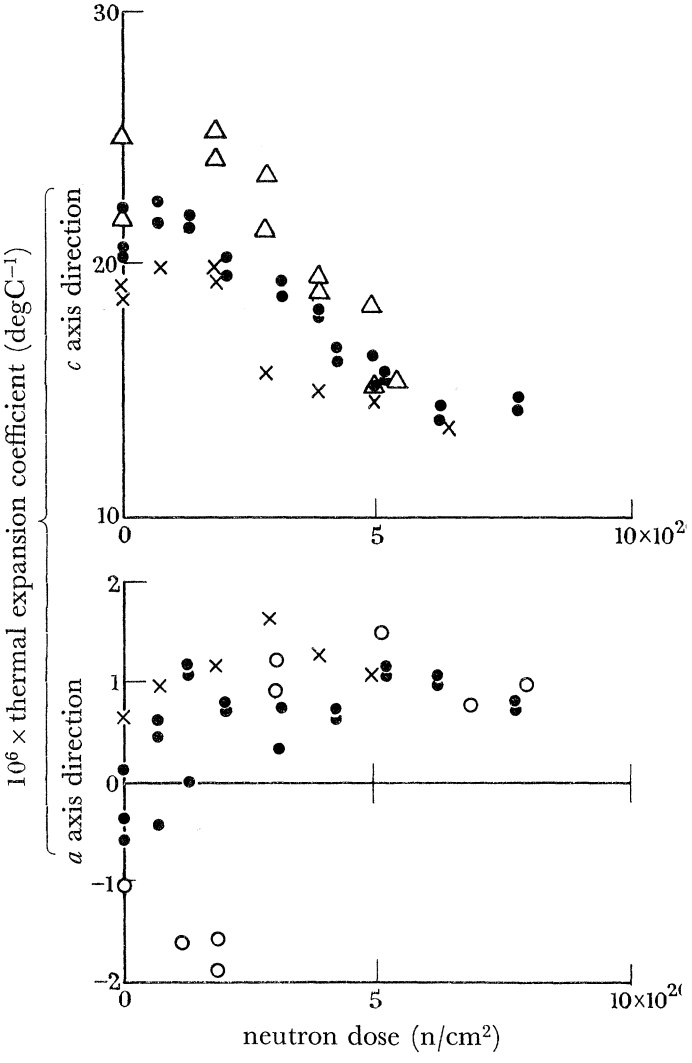

FIGURE 7. Comparison of changes in thermal expansi coefficients in α, β and γ materials irradiated at 170 ° ×, α material; ○ (plate 1), ● (plate 4), β materi △, γ material.

The basal plane contraction is attributed to the presence of vacancies in the layer planes, together with a Poisson ratio contraction (Nelson & Riley 1945) amounting to about 0·07 of the c axis lattice expansion. The contraction due to single vacancies is expected to be *ca.* $-0{\cdot}1\,C_v$ (Kelly 1965) where C_v is the vacancy concentration, and this effect together with the Poisson effect leads to a strain in the 'a' direction of

$$\epsilon_a = -0{\cdot}1C_v - 0{\cdot}07\,\Delta c/c. \qquad (2)$$

At the highest dose at 200 °C this would require a vacancy concentration of *ca.* 50 % in order to explain the observed contraction, which is clearly unacceptable on lattice stability grounds. The Poisson effect and the distortion around single vacancies should yield lattice parameter changes in agreement with directly measured length changes.

It is extremely unlikely that any interstitial defect could produce the large difference by buckling the layer planes and it is thus necessary to postulate some other type of defect to explain the high dose contraction at 200 °C and the contraction at higher temperature.

The nature of this defect may be further discussed if we examine the volume changes, $\Delta V/V$, of the crystal/unit dose γ; that is

$$\frac{1}{V}\frac{\mathrm{d}V}{\mathrm{d}\gamma} \simeq \frac{\mathrm{d}\epsilon_c}{\mathrm{d}\gamma} + 2\frac{\mathrm{d}\epsilon_a}{\mathrm{d}\gamma}, \tag{3}$$

which can be written

$$= \frac{\mathrm{d}\epsilon_c}{\mathrm{d}\gamma}(1-2\delta).$$

The quantities $\mathrm{d}\epsilon_c/\mathrm{d}\gamma$ and $\delta = -(\mathrm{d}\epsilon_a/\mathrm{d}\gamma)/(\mathrm{d}\epsilon_c/\mathrm{d}\gamma)$ for the 200 °C irradiation are presented in figure 8. In particular, it must be noted that $\delta \simeq 0{\cdot}5$ at the highest dose and thus the crystal is changing shape but not volume. It has already been shown that essentially all the growth at these doses is due to large clusters and thus $\mathrm{d}\epsilon_c/\mathrm{d}\gamma = \mathrm{d}C_d/\mathrm{d}\gamma$, and thus if $\delta = 0{\cdot}5$,

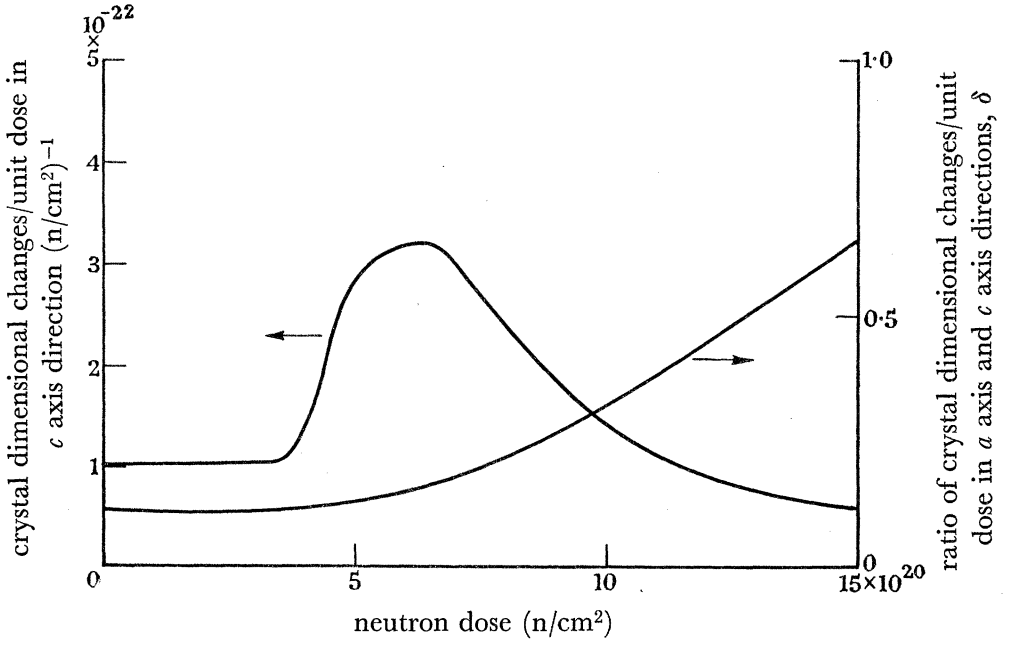

FIGURE 8. Dependence on dose at 200 °C of the dimensional change/unit dose in the c axis direction and the ratio of the crystal dimensional changes/unit dose in the a axis and c axis directions.

$\mathrm{d}\epsilon_a/\mathrm{d}\gamma = -0{\cdot}5\,\mathrm{d}C_d/\mathrm{d}\gamma$. It is reasonable to assume that the contraction is due to the parent vacancies of the interstitial atoms which contribute to growth in dose $\mathrm{d}\gamma$. We must therefore conclude that these vacancies are contributing their full cross-sectional area in the basal plane to contraction of the basal plane. The only defect conceived by the authors with this property is an irregular line of vacancies in the layer planes which collapses when it reaches a certain length. The immobility of the vacancies in this temperature range leads to the conclusion that these lines must either be formed on some existing line defect or created by random vacancy formation at sites adjacent to existing vacancies. The former possibility is unlikely since the perfection of the material does not affect the results at 170 °C.

PHILOSOPHICAL TRANSACTIONS OF THE ROYAL SOCIETY A MATHEMATICAL, PHYSICAL & ENGINEERING SCIENCES

In further consideration of the second postulated mechanism, it appears likely that the lines grow only at their ends by adjacent displacements. If this is the case, then the contraction rate is given by

$$\frac{\mathrm{d}\epsilon_a}{\mathrm{d}\gamma} = -\frac{G_0}{\phi}\frac{N}{N_0}Z, \tag{4}$$

where G_0 (atoms atom^{-1} s^{-1}) is the atomic displacement rate in flux ϕ, N_0 is the number of atoms/cm^3, Z is the number of atoms immediately adjacent to the end of a line and N is the number of lines/unit volume. The presence of such lines would explain the high values of δ and also the difference between the fractional change in lattice parameter $\Delta a/a$ and the basal plane contraction. The argument is similar to that for the large interstitial clusters in that the lattice strain is confined to the ends of the line and is less than the crystallite contraction. It is also notable that the reformation of co-valent bonds across the line should reduce the contribution of this defect to other property changes and annealing studies have confirmed this (Kelly, Martin, Dolby, Price & Smith, to be published).

The same type of defect must also be formed at the higher irradiation temperatures to explain the increasing ratio of basal plane contraction to c axis growth shown in figure 3. Equation (4) may be used to estimate the value of N at each temperature. In the 200 °C irradiation at the highest dose the contraction rate is $0{\cdot}45 \times 10^{-22}$/n cm^{-2} which, assuming a flux of 4×10^{13} n cm^{-2} s^{-1}, yields $N \sim 10^{21}$ cm^{-3}. In the higher temperature irradiations $N \sim 10^{20}$ cm^{-3}. If at 200 °C the difference between the lattice parameter change $\Delta a/a$ and the basal plane contraction is attributed to these line defects then each must contain *ca.* 6 vacancies, which is not unreasonable considering the approximate nature of equation (4).

The changes in the principal thermal expansion coefficients of the graphite crystal due to the presence of irradiation induced defects at the lower irradiation temperatures are associated with large changes in the crystal lattice parameters. The c axis thermal expansion coefficient is associated with the accommodation of thermal vibrations normal to the layers. Since the presence of the irradiation defects increases the c axis lattice parameter, this could permit a partial accommodation of the change of vibration amplitude with temperature, together with a corresponding decrease in the c axis thermal expansion coefficient. Such a decrease is not immediately observed however; a change of lattice parameter $\Delta c/c$ equal to 3 % has to occur before any decrease in α_c is observed. This may be due to a decreasing interaction between layers which initially allows an increased vibration amplitude. However, the vibration amplitude of the layers will eventually be limited by the bond bending forces rather than those due to adjacent layers, and at this stage the reduction of α_c becomes noticeable. The saturation of changes in the lattice parameter coincides with the termination of changes in α_c, in agreement with these considerations. In the higher temperature irradiations no lattice parameter changes of any magnitude and no changes in crystal thermal expansion coefficient have so far been observed. The a axis thermal expansion coefficient changes from a small negative value to a small positive value at the lower irradiation temperatures. It is difficult to explain this change in detail. It is partly due to the changes in bond strength and vibration frequencies of the layer planes due to the lattice vacancies, but the major part of the effect probably results from a decrease in the Poisson strain as α_c decreases (cf. Nelson & Riley 1945).

PHILOSOPHICAL TRANSACTIONS OF THE ROYAL SOCIETY A MATHEMATICAL, PHYSICAL & ENGINEERING SCIENCES

The application of these data to the analysis of dimensional changes in polycrystalline graphites is discussed in the succeeding paper.

The authors wish to express their gratitude to Dr R. J. Diefendorf and Dr J. T. Clarke of the U.S. General Electric Company for the γ graphite samples, and High Temperature Materials Inc. U.S.A. for the α material.

The X-ray measurements in table 1 are published by permission of Chemical Engineering Division, A.E.R.E., and the General Electric Company, Wembley (Dr H. P. Rooksby).

References

Agranovich, V. M. & Semenov, L. P. 1964 *J. Nucl. Energy*, parts A/B, **11**, 141.

Bell, J. C., Bridge, H., Cottrell, A. H., Greenough, G. B., Reynolds, W. N. & Simmons, J. H. W. 1962 *Phil. Trans.* A, **254**, 361.

Blackman, L. C., Saunders, G. A. & Ubbelohde, A. R. 1961 *Proc. Roy. Soc.* A, **264**, 19.

Bragg, R. H., Crooks, D. D., Fenn, R. W. & Hammond, L. W. 1964 *Carbon*, **1**, 171.

Bridge, H., Kelly, B. T. & Nettley, P. T. 1964 *Carbon*, **2**, 83.

Brocklehurst, J. E. & Weeks, J. C. 1963 *J. Nucl. Mater.* **9**, 197.

Brown, A. R. G., Watt, W., Powell, R. W. & Tye, R. P. 1956 *Br. J. Appl. Phys.* **7**, 73.

Diefendorf, R. J. 1960 *Proc. Fourth Biennial Conference on Carbon*, p. 483. London: Pergamon Press.

Entwisle, F. 1962 *Phys. Lett.* **2**, no. 5, 236.

Freise, E. J. & Kelly, A. 1961 *Proc. Roy. Soc.* A, **264**, 269.

Goggin, P. R., Henson, R. W., Perks, A. J. & Reynolds, W. N. 1964 *Carbon*, **1**, 189.

Kellett, E. A., Wallace, C. A. & Richards, B. P. 1962–64 *G.E.C. Rep. nos.* 14, 516C and 14,320C. General Electric Co. Ltd., London.

Kelly, B. T. 1965 *Proc. S.C.I. Conference on Industrial Carbons and Graphites*. London. To be published.

Kelly, B. T., Gray, B. S., Martin, W. H., Howard, V. C. & Sørensen, H. 1965 *Proc. S.C.I. Conference on Industrial Carbons and Graphites*. London. To be published.

Kelly, B. T., Jones, D. & James, A. 1962 *J. Nucl. Mater.* **7**, 279.

Martin, W. H. & Clare, D. M. 1964 *Nucl. Sci. Engng*, **18**, 468.

McFarlane, A. A. 1965 *J. Sci. Instrum.* **42**, 24.

Nelson, J. B. & Riley, H. L. 1945 *Proc. Phys. Soc.* **57**, 477.

Primak, W. & Fuchs, L. H. 1954 *Phys. Rev.* **95**, 22.

Reynolds, W. N. & Thrower, P. A. 1963 *Radiation damage in reactor materials*, p. 553. I.A.E.A.

Simmons, J. H. W. 1957 *Proc. Third Conference on Carbon*, p. 559. London: Pergamon Press.

Simmons, J. H. W. 1965 *Radiation damage in graphite*, chap. 2. Oxford: Pergamon Press.

Simmons, J. H. W., Kelly, B. T., Nettley, P. T. & Reynolds, W. N. 1964 *Proc. Third Geneva Conf. on the Peaceful Uses of Atomic Energy*, A/CONF. 28/P/163.

Simmons, J. H. W. & Reynolds, W. N. 1962 Uranium and graphite, *Monogr. Inst. Metals, London*, no. 27, p. 75.

Smith, A. W. 1956 *Phys. Rev.* **95**, 1095.

Tarpinian, A. 1962 *J. Appl. Phys.* **33**, 3386.

Thrower, P. A. 1964 *J. Nucl. Mater.* **12**, 56.

Ubbelohde, A. R. & Lewis, F. A. 1960 *Graphite and its crystal compounds*. London: Oxford University Press.

PHILOSOPHICAL TRANSACTIONS OF THE ROYAL SOCIETY A MATHEMATICAL, PHYSICAL & ENGINEERING SCIENCES

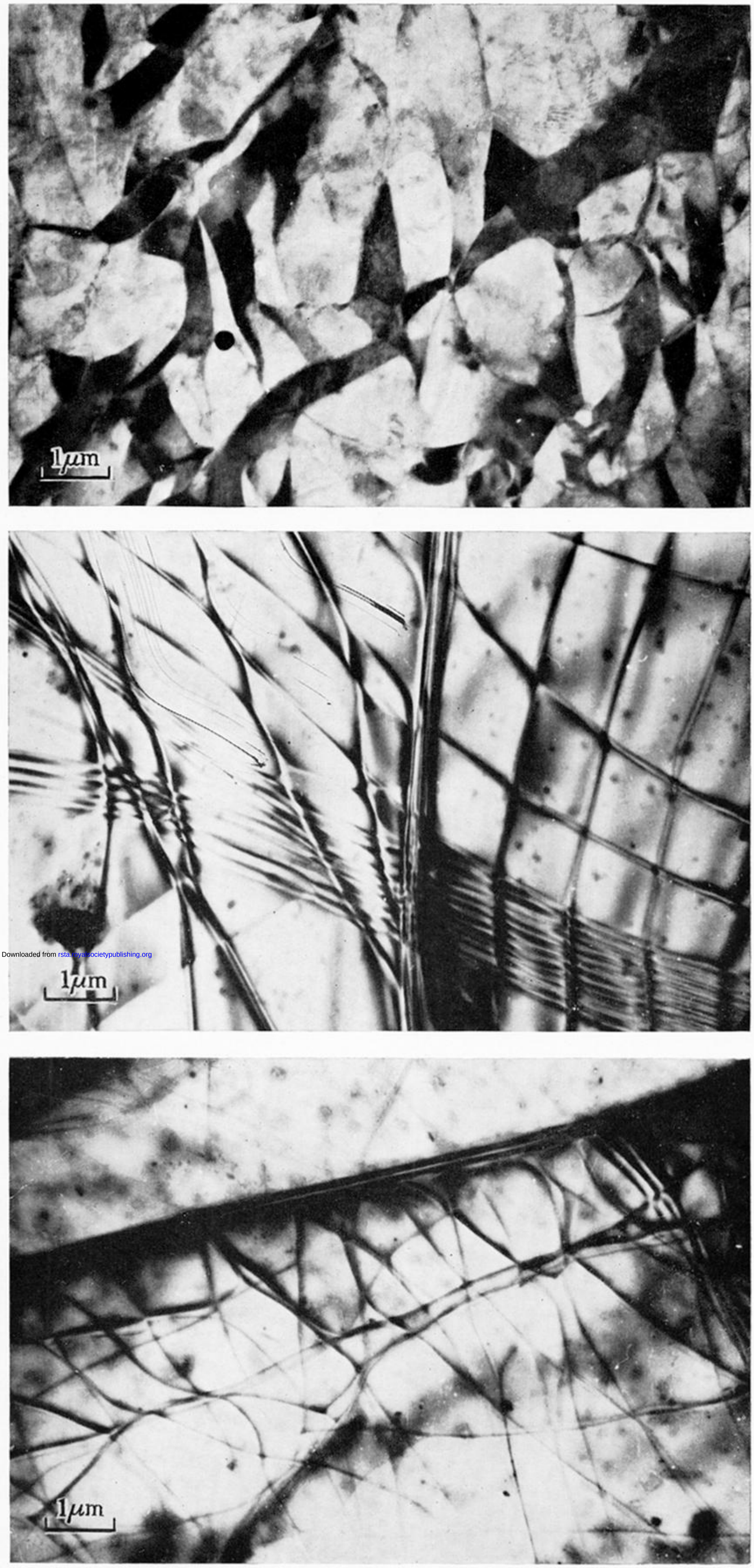

(A) β type material

(B) γ type material

(C) Ticonderoga flake graphite

FIGURE 1. Transmission electron micrographs of pyrolytic and monocrystalline graphite. (Magn. $\times 8700$). Micrographs (B) and (C) show dislocation networks lying in the basal planes.